

1           Back to Einstein: burial-induced ~~three-range~~  
2           three-range diffusion in fluvial sediment transport

3           J. Kevin Pierce <sup>1</sup>and Marwan A. Hassan<sup>1</sup>

4                           <sup>1</sup>Department of Geography  
5                           University of British Columbia

6           **Key Points:**

- 7           • Random walk model describes coarse gravel tracers ~~diffusing through~~ spreading  
8           out within a river as they gradually become buried  
9           • Interchange of grains between motion, surface rest, and burial states generates  
10          three diffusion ranges as the observation time increases  
11          • Sediment burial dominates long-time properties and exhumation may develop a  
12          fourth “geomorphic” range of tracer diffusion

## Abstract

Individual grains move through gravel bed rivers in cycles of motion and rest with variable characteristics, so tracer grains spread apart and diffuse as they transport downstream in a type of diffusion. Experiments and Newtonian simulations have demonstrated nuanced diffusion characteristics, with Tracer experiments demonstrating at least three distinct ranges of behavior as the observation time of tracers increases and each range exhibiting a different spreading rate. Although these observations are nearly 20 years old, no physical model has been developed to describe them, leaving us uncertain of diffusion ranges as observation times increase, with different spreading rates in each range. Up till now, the generating processes of these ranges remain unclear. In this work, we develop the first physical model describing three bedload diffusion ranges by incorporating sediment a random walk model of individual bedload trajectories including motion, rest, and burial into a random walk concept of individual bedload trajectories processes. The model describes three bedload diffusion ranges that terminate in a fourth non-diffusive range when all tracers become buried. Using the model, we attribute multiple bedload diffusion ranges to three-range tracer diffusion to the interplay between motion, rest, and burial processes, and we relate the multi-range diffusion characteristics to measurable transport parameters the timescales of these processes.

## 1 Introduction

Many environmental problems including channel morphology (Hassan & Bradley, 2017), contaminant transport (Macklin et al., 2006), and aquatic habitat restoration (Gaeuman, Stewart, Schmandt, & Pryor, 2017) rely on our ability to predict the diffusion characteristics of coarse sediment tracers in river channels. Diffusion is quantified by the time dependence of the positional variance  $\sigma_x^2$  of a group of tracers. With the scaling  $\sigma_x^2 \propto t$ , the diffusion is said to be normal, since this is found in the classic problems (Taylor, 1920). However, with the scaling  $\sigma_x^2 \propto t^\gamma$  with  $\gamma \neq 1$ , the diffusion is said to be anomalous (Sokolov, 2012), with  $\gamma > 1$  defining super-diffusion and  $\gamma < 1$  defining sub-diffusion (Metzler & Klafter, 2000). Einstein (1937) developed one of the earliest models of bedload diffusion to describe a series of flume experiments (Ettema & Mutel, 2014). Interpreting individual bedload trajectories as a sequence of random steps and rests, Einstein originally concluded that a group of bedload tracers undergoes normal diffusion.

More recently, Nikora et al. realized coarse sediment tracers can show either normal or anomalous diffusion depending on the length of time they have been tracked (Nikora, Habersack, Huber, & McEwan, 2002; Nikora, Heald, Goring, & McEwan, 2001). From numerical simulations and experimental data, Nikora et al. discerned “at least three” scaling ranges  $\sigma_x^2 \propto t^\gamma$  as the observation time increased. They associated the first range with “local” timescales less than the interval between subsequent collisions of moving grains with the bed, the second with “intermediate” timescales less than the interval between successive resting periods of grains, and the third with “global” timescales composed of many intermediate timescales. Nikora et al. proposed super-diffusion in the local range, anomalous or normal diffusion in the intermediate range, and sub-diffusion in the global range. They attributed these ranges to “differences in the physical processes which govern the local, intermediate, and global trajectories” of grains (Nikora et al., 2001), and they called for a physically based model to explain the diffusion characteristics (Nikora et al., 2002).

Experiments support the Nikora et al. conclusion of multiple scaling ranges (S. Fathel, Furbish, & Schmeeckle, 2016; Martin, Jerolmack, & Schumer, 2012), but they do not provide consensus on the expected number of ranges or their scaling properties. This lack of consensus probably stems from resolution issues. For example,

experiments have tracked only moving grains, resolving the local range (S. Fathel et al., 2016; Furbish, Ball, & Schmeeckle, 2012; Furbish, Fathel, Schmeeckle, Jerolmack, & Schumer, 2017); grains resting on the bed surface between movements, resolving the intermediate range (Einstein, 1937; Nakagawa & Tsujimoto, 1976; Yano, 1969); grains either moving or resting on the bed surface, likely resolving local and intermediate ranges (Martin et al., 2012); or grains resting ~~between subsequent on the surface after~~ floods, likely resolving the global range (Bradley, 2017; Phillips, Martin, & Jerolmack, 2013). At long timescales, a significant fraction of tracers bury under the bed surface (Ferguson, Bloomer, Hoey, & Werritty, 2002; Haschenburger, 2013; Hassan, Church, & Schick, 1991; Hassan, Voepel, Schumer, Parker, & Fraccarollo, 2013; Papangelakis & Hassan, 2016), meaning burial dominates long term diffusion characteristics (Bradley, 2017; Martin, Purohit, & Jerolmack, 2014; Voepel, Schumer, & Hassan, 2013), possibly at global or even longer “geomorphic” timescales (Hassan & Bradley, 2017) than Nikora et al. originally considered. As a result, three diffusion ranges can be identified by patching together multiple datasets (Nikora et al., 2002; Zhang, Meerschaert, & Packman, 2012), but they are not resolved by any one dataset.

Newtonian bedload trajectory models also show multiple diffusion ranges, although they also do not provide consensus on the expected number of ranges or their scaling properties. The majority of these models predict two ranges of diffusion (local and intermediate) without predicting a global range. Among these, Nikora et al. (2001) used synthetic turbulence (Kraichnan, 1970) with a discrete element method for the granular phase (Cundall & Strack, 1979); Bialik, Nikora, and Rowiński (2012) used synthetic turbulence with a random collision model (Sekine & Kikkawa, 1992); and Fan, Singh, Guala, Foufoula-Georgiou, and Wu (2016) used a Langevin equation with probabilistic rests. To our knowledge, only Bialik, Nikora, Karpiński, and Rowiński (2015) have claimed to capture all three ranges from a ~~semi-Newtonian~~ Newtonian approach. They incorporated a second resting mechanism into their earlier model (Bialik et al., 2012), implicitly suggesting that three diffusion ranges could result from two distinct timescales of sediment rest. However, Newtonian approaches have not evaluated the effect of sediment burial on tracer diffusion, probably due to the long simulation timescales required.

Random walk bedload diffusion models constructed in the spirit of Einstein (1937) provide an alternative to the Newtonian approach and can include a second timescale of rest by incorporating sediment burial. Einstein originally modeled bedload trajectories as instantaneous steps interrupted by durations of rest lying on statistical distributions (Hassan et al., 1991), but this generates only one range of normal diffusion (Einstein, 1937; Hubbell & Sayre, 1964; Nakagawa & Tsujimoto, 1976). Recently, researchers have generalized Einstein’s model in a few different ways to describe multiple diffusion ranges. Lisle et al. (1998) and Lajeunesse, Devauchelle, and James (2018) promoted Einstein’s instantaneous steps to motion intervals with random durations and a constant velocity, providing two diffusion ranges – local and intermediate. Wu, Foufoula-Georgiou, et al. (2019) retained Einstein’s instantaneous steps but included the possibility that grains can become permanently buried as they rest on the bed, also providing two diffusion ranges – intermediate and global. ~~Although no Einstein-type model of three bedload diffusion ranges has been developed, these~~ These earlier works suggest the minimal required components ~~are to model three bedload diffusion ranges:~~ (1) exchange between motion and rest intervals and (2) the sediment burial process.

In this study, we incorporate these two components into Einstein’s original approach to describe three diffusion ranges with a physically based model, as called for by Nikora et al. (2002). Einstein was a giant in river geophysics and fostered an entire paradigm of research leveraging and generalizing his stochastic methods (Gordon, Carmichael, & Isackson, 1972; Hubbell & Sayre, 1964; Nakagawa & Tsujimoto, 1976; Paintal, 1971; Yang & Sayre, 1971; Yano, 1969). Einstein’s model can be viewed as

a pioneering application of the continuous time random walk (CTRW) developed by Montroll and Weiss (1965) in condensed matter physics to describe the diffusion of charge carriers in solids. To incorporate motion intervals and sediment burial, we utilize the multi-state CTRW developed by Weiss (1976, 1994) that extends the CTRW of Montroll and Weiss (1965). Below, we develop and solve the model in section 2, ~~and~~ . Then, we discuss the predictions of our model, present its implications for local, intermediate, and global ranges of bedload diffusion, and suggest next steps for bedload diffusion research in sections 3 and 4.

## 2 Bedload trajectories as a multi-state random walk

### 2.1 Model assumptions

We construct a three-state random walk where the states are motion, surface rest, and burial, and we label these states as  $i = 2$  (motion),  $i = 1$  (rest), and  $i = 0$  (burial). Our target is the probability distribution  $p(x, t)$  to find a grain at position  $x$  and time  $t$  if we know it started with the initial distribution  $p(x, 0) = \delta(x)$ . We characterize times spent moving or resting on the surface by exponential distributions  $\psi_2(t) = k_2 e^{-k_2 t}$  and  $\psi_1(t) = k_1 e^{-k_1 t}$ , since numerous experiments show thin-tailed distributions for these quantities (Ancey, Böhm, Jodeau, & Frey, 2006; Einstein, 1937; S. L. Fathel, Furbish, & Schmeeckle, 2015; Martin et al., 2012; Roseberry, Schmeeckle, & Furbish, 2012). We expect our conclusions will not be contingent on the specific distributions chosen, since all thin-tailed distributions provide similar diffusion characteristics in random walks (Weeks & Swinney, 1998; Weiss, 1994). We consider grains in motion to have characteristic velocity  $v$  (Lajeunesse et al., 2018; Lisle et al., 1998), and we model burial as long lasting enough to be effectively permanent (Wu, Foufoula-Georgiou, et al., 2019), with grains resting on the surface having a probability per unit time  $\kappa$  to become buried, meaning  $\Phi(t) = e^{-\kappa t}$  represents the probability that a grain is not buried after resting for a time  $t$ , while  $1 - \Phi(t)$  represents the probability that it is buried. We specify the initial conditions with probabilities  $\theta_1$  and  $\theta_2$  to be in rest and motion at  $t = 0$ , and we require  $\theta_1 + \theta_2 = 1$  for normalization.

### 2.2 Governing equations

Using these assumptions, we derive the governing equations for the set of probabilities  $\omega_{ij}(x, t)$  that a transition occurs from state  $i$  to state  $j$  at position  $x$  and time  $t$  using the statistical physics approach to multi-state random walks (Schmidt, Sagués, & Sokolov, 2007; Weeks & Swinney, 1998; Weiss, 1994). Denoting by  $g_{ij}(x, t)$  the probability for a particle to displace by  $x$  in a time  $t$  within the state  $i$  before it transitions to the state  $j$ , the transition probabilities  $\omega_{ij}(x, t)$  sum over all possible paths to the state  $i$  from previous locations and times:

$$\omega_{ij}(x, t) = \theta_i g_{ij}(x, t) + \sum_{k=0}^2 \int_0^x dx' \int_0^t dt' \omega_{ki}(x', t') g_{ij}(x - x', t - t'). \quad (1)$$

Defining another set of probabilities  $G_i(x, t)$  that a particle displaces by a distance  $x$  in a time  $t$  within the state  $i$  and possibly remains within the state, we perform a similar sums over paths for the probabilities to be in the state  $i$  at  $x, t$ :

$$p_i(x, t) = \theta_i G_i(x, t) + \sum_{k=0}^2 \int_0^x dx' \int_0^t dt' \omega_{ki}(x', t') G_i(x - x', t - t'). \quad (2)$$

Finally, the overall probability to be at position  $x$  at time  $t$  is

$$p(x, t) = \sum_{k=0}^2 p_k(x, t) \quad (3)$$

This joint density is completely determined from the solutions of equations (1-2). We only need to specify the distributions  $g_{ij}$  and  $G_i$ .

### 2.3 Joint probability distribution

We construct these distributions from the assumptions described in section 2.1. Since particles resting on the bed surface bury in a time  $t$  with probability  $\Phi(t)$ , and resting times are distributed as  $\psi_1(t)$ , we obtain  $g_{12}(x, t) = \delta(x)k_1e^{-k_1t}e^{-\kappa t}$  and  $g_{10}(x, t) = \delta(x)k_1e^{-k_1t}(1 - e^{-\kappa t})$ . Since motions have velocity  $v$  for times distributed as  $\psi_2(t)$ , we have  $g_{21}(x, t) = \delta(x - vt)k_2e^{-k_2t}$ . Since burial is quasi-permanent, all other  $g_{ij} = 0$ . The  $G_i$  are constructed in the same way except using the cumulative probabilities  $\int_t^\infty dt' \psi_i(t') = e^{-k_i t}$ , since these characterize motions and rests that are ongoing (Weiss, 1994). We obtain  $G_1(x, t) = \delta(x)e^{-k_1 t}$  and  $G_2(x, t) = \delta(x - vt)e^{-k_2 t}$ .

To solve equations (1-2) with these  $g_{ij}$  and  $G_i$ , we take Laplace transforms in space and time ( $x, t \rightarrow \eta, s$ ) using a method similar to Weeks and Swinney (1998) to unravel the convolution structure of these equations, eventually obtaining

$$\tilde{p}(\eta, s) = \frac{1}{s} \frac{(s + \kappa + k')s + \theta_1(s + \kappa)\eta v + \kappa k_2}{(s + \kappa + k_1)\eta v + (s + \kappa + k')s + \kappa k_2}, \quad (4)$$

where  $k' = k_1 + k_2$ . Inverting this result using known Laplace transforms (Arfken, 1985; Prudnikov et al., 1986) obtains

$$p(x, t) = \theta_1 \left[ 1 - \frac{k_1}{\kappa + k_1} \frac{1 - e^{-(\kappa + k_1)t} \delta(x) + \frac{1}{v} e^{-\Omega \tau - \xi} \theta_1 k_1 \mathcal{I}_0 2\sqrt{\xi \tau} + k_2 \sqrt{\frac{\tau}{\xi}} \mathcal{I}_1 2\sqrt{\xi \tau} + \theta_2 k_1 \delta(\tau) + k_2 \mathcal{I}_0 2\sqrt{\xi \tau} + k_1 \sqrt{\frac{\xi}{\tau}} \mathcal{I}_1 2\sqrt{\xi \tau}} \right] \quad (5)$$

for the joint distribution that a tracer is found at position  $x$  at time  $t$ . This result generalizes the earlier results of Lisle et al. (1998) and Einstein (1937) to include sediment burial. In this equation, we used the shorthand notations  $\xi = k_2 x/v$ ,  $\tau = k_1(t - x/v)$ , and  $\Omega = (\kappa + k_1)/k_1$  (Lisle et al., 1998). The  $\mathcal{I}_\nu$  are modified Bessel functions of the first kind and the  $\mathcal{Q}_\mu$  are generalized Marcum Q-functions defined by  $\mathcal{Q}_\mu(x, y) = \int_0^y e^{-z-x} (z/x)^{(\mu-1)/2} \mathcal{I}_{\mu-1}(2\sqrt{xz}) dz$  and originally devised for radar detection theory (Marcum, 1960; Temme, 1996). ~~Burial generates the~~ The Marcum Q-functions ~~, since derive from the burial process.~~ Since we assumed resting grains could bury with an exponential probability ~~, while the rest while the resting~~ probability follows a modified Bessel distribution (Einstein, 1937; Lisle et al., 1998), burial develops the Q-function convolution structure.

Figure 1 depicts the distribution (5) alongside simulations generated by a direct method based on evaluating the cumulative transition probabilities between states on a small timestep (Barik, Ghosh, & Ray, 2006). When grains do not become buried, as in panel (a) of figure 1, the distribution becomes Gaussian-like at relatively large observation times, exemplifying normal diffusion and satisfying the central limit theorem. When grains become buried, as in panel (b) of figure 1, the Q-function terms prevent the distribution from approaching a Gaussian at large timescales, exemplifying anomalous diffusion (Weeks & Swinney, 1998) and violating the central limit theorem (Metzler & Klafter, 2000; Schumer, Meerschaert, & Baeumer, 2009).

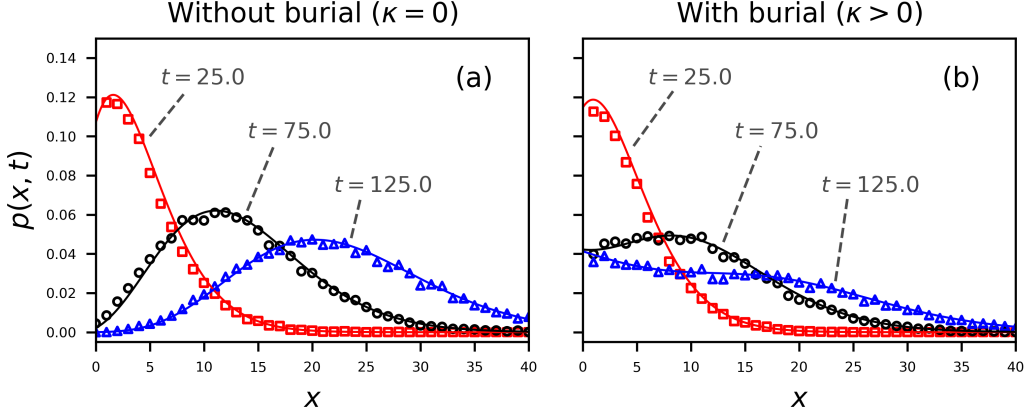


**Figure 1.** Joint distributions for a grain to be at position  $x$  at time  $t$  are displayed for the choice  $k_1 = 0.1$ ,  $k_2 = 1.0$ ,  $v = 2.0$ . Grains are considered initially at rest ( $\theta_1 = 1$ ,  $\theta_2 = 0$ ). The solid lines are the analytical distribution in equation (5), while the points are numerically simulated, showing the correctness of our derivations. Colors pertain to different times. Units are unspecified, since we aim to demonstrate the general characteristics of  $p(x, t)$ . Panel (a) shows the case  $\kappa = 0$  – no burial. In this case, the joint distribution tends toward Gaussian at large times (Einstein, 1937; Lisle et al., 1998). Panel (b) shows the case when grains have rate  $\kappa = 0.01$  to become buried while resting. Because of burial, the joint distribution tends toward a more uniform distribution than Gaussian.

## 2.4 Positional variance

To obtain an analytical formula for tracers diffusing downstream while they gradually become buried, we derive the first two moments of position by taking derivatives with respect to  $\eta$  of the Laplace space distribution (4) using an approach similar to Shlesinger (1974) and Weeks and Swinney (1998), and we use these to calculate the positional variance  $\sigma_x^2 = \langle x^2 \rangle - \langle x \rangle^2$ . The first two moments are

$$\langle x(t) \rangle = A_1 e^{(b-a)t} + B_1 e^{-(a+b)t} + C_1, \quad (6)$$

$$\langle x^2(t) \rangle = A_2(t) e^{(b-a)t} + B_2(t) e^{-(a+b)t} + C_2, \quad (7)$$

so the variance is

$$\sigma_x^2(t) = A(t) e^{(b-a)t} + B(t) e^{-(a+b)t} + C(t). \quad (8)$$

In these equations,  $a = (\kappa + k_1 + k_2)/2$  and  $b = \sqrt{a^2 - \kappa k_2}$  are effective rates having dimensions of inverse time, while the  $A$ ,  $B$ , and  $C$  factors are provided in table 1.

The positional variance (8) is plotted in figure 2 for conditions  $\theta_1 = 1$  and  $k_2 \gg k_1 \gg \kappa$ . We interpret “ $\gg$ ” to mean “of at least an order of magnitude greater”. These conditions are most relevant to tracers in gravel-bed rivers, since they ~~mean all~~ represent that grains are initially at rest (Hassan et al., 1991; Wu, Foufoula-Georgiou, et al., 2019), motions are typically much shorter than rests (Einstein, 1937; Hubbell & Sayre, 1964), and burial requires a much longer time than typical rests (Ferguson & Hoey, 2002; Haschenburger, 2013; Hassan & Church, 1994). Figure 2 demonstrates that under these conditions the variance (8) shows three diffusion ranges with approximate power law scaling ( $\sigma_x^2 \propto t^\gamma$ ) that we identify as the local, intermediate, and global ranges proposed by Nikora et al., followed by a fourth range of no diffusion ( $\sigma_x^2 = \text{const}$ ) stemming from the burial of all tracers. We suggest to call the fourth range geomorphic, since any further transport in this range can occur only if scour

**Table 1.** Abbreviations used in the expressions of the mean (6), second moment (7) and variance (8) of bedload tracers.

---

$A_1 = \frac{v}{2b} \left[ \theta_2 + \frac{k_1 + \theta_2 \kappa}{b - a} \right]$
$B_1 = -\frac{v}{2b} \left[ \theta_2 - \frac{k_1 + \theta_2 \kappa}{a + b} \right]$
$C_1 = -\frac{v}{2b} \left[ \frac{k_1 + \theta_2 \kappa}{b - a} + \frac{k_1 + \theta_2 \kappa}{a + b} \right]$
$A_2(t) = \frac{v^2}{2b^3} \left[ (bt - 1)[k_1 + \theta_2(2\kappa + k_1 + b - a)] + \theta_2 b + \frac{(\kappa + k_1)(\theta_2 \kappa + k_1)}{(b - a)^2} [(bt - 1)(b - a) - b] \right]$
$B_2(t) = \frac{v^2}{2b^3} \left[ (bt + 1)[k_1 + \theta_2(2\kappa + k_1 - a - b)] + \theta_2 b - \frac{(\kappa + k_1)(\theta_2 \kappa + k_1)}{(a + b)^2} [(bt + 1)(a + b) + b] \right]$
$C_2 = \frac{v^2}{2b^3} (\kappa + k_1)(\theta_2 \kappa + k_1) \left[ \frac{2b - a}{(b - a)^2} + \frac{a + 2b}{(a + b)^2} \right]$
$A(t) = A_2(t) - 2A_1C_1 - A_1^2 \exp[(b - a)t]$
$B(t) = B_2(t) - 2B_1C_1 - B_1^2 \exp[-(a + b)t]$
$C(t) = C_2 - C_1^2 - 2A_1B_1 \exp[-2at]$

---

re-exposes buried grains to the flow (Martin et al., 2014; Nakagawa & Tsujimoto, 1980; Voepel et al., 2013; Wu, Singh, Fu, & Wang, 2019).

## 2.5 Diffusion exponents

Two limiting cases of equation (8) provide the scaling exponents  $\gamma$  of the diffusion  $\sigma_x^2 \propto t^\gamma$  in each range. Limit (1) represents times so short a negligible amount of sediment burial has occurred,  $t \ll 1/\kappa$ , while limit (2) represents times so long motion intervals appear as instantaneous steps of mean length  $l = v/k_2$ ,  $1/k_2 \rightarrow 0$  while  $v/k_2 = \text{constant}$ . Limit (1) provides local exponent  $2 \leq \gamma \leq 3$  depending on the initial conditions  $\theta_i$ , and intermediate exponent  $\gamma = 1$ . If grains start in motion or rest exclusively, meaning one  $\theta_i = 0$ , the local exponent is  $\gamma = 3$ , while if grains start in a mixture of motion and rest states, meaning neither  $\theta_i$  is zero, the local exponent is  $\gamma = 2$ . Limit (2) provides global exponent  $1 \leq \gamma \leq 3$  depending on the relative importance of  $\kappa$  and  $k_1$ . In the extreme  $k_1/\kappa \ll 1$ , we find  $\gamma = 1$  in the global range, while in the opposite extreme  $k_1/\kappa \rightarrow \infty$  we find  $\gamma = 3$ . We summarize when  $k_2 \gg k_1 \gg \kappa$  so all three diffusion ranges exist, equation (8) implies:

1. local range super-diffusion with  $2 < \gamma < 3$  depending on whether grains start from purely motion or rest ( $\gamma = 3$ ) or from a mixture of both states ( $\gamma = 2$ ),
2. intermediate range normal diffusion  $\gamma = 1$  independent of model parameters, and
3. global range super-diffusion  $1 < \gamma < 3$  depending on whether burial happens relatively slowly ( $\gamma \rightarrow 1$ ) or quickly ( $\gamma \rightarrow 3$ ) compared to surface resting times.

Finally, the burial of all tracers generates a geomorphic range of no diffusion.

## 3 Discussion

### 3.1 Local and intermediate ranges with comparison to earlier work

We extended Einstein (1937) by including motion and burial processes in a multi-state random walk (Weeks & Swinney, 1998; Weiss, 1994) to demonstrate that a group of bedload tracers moving downstream while gradually becoming buried will gener-



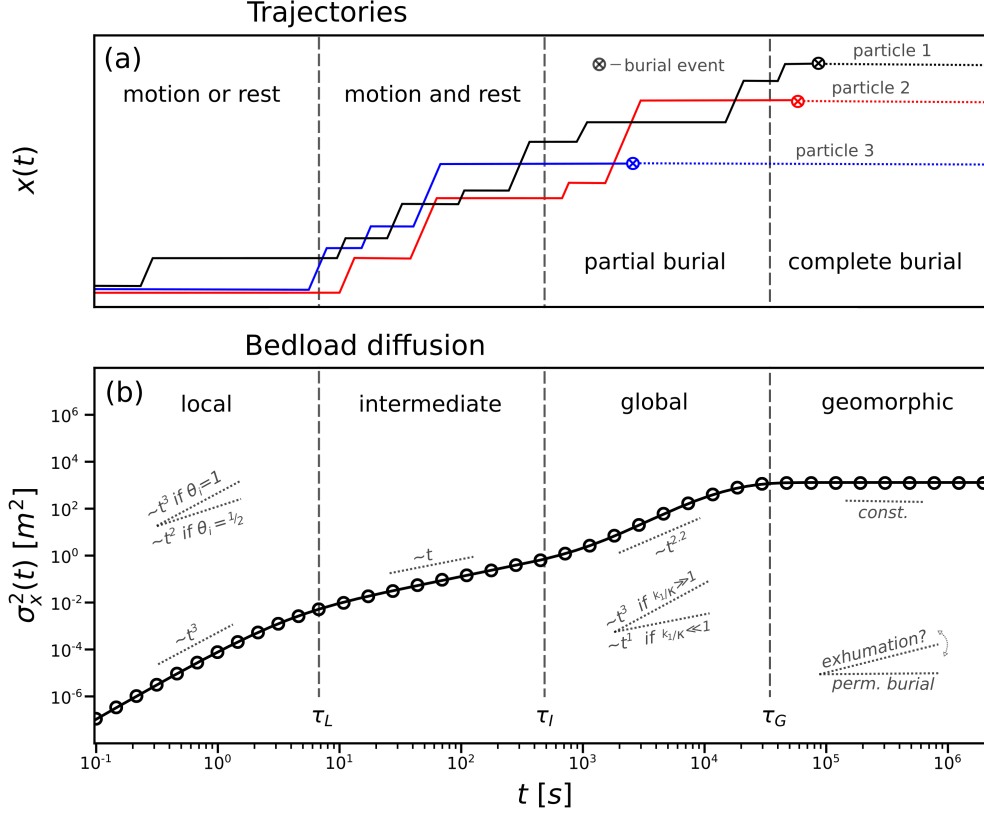


**Figure 2.** Panel (a) sketches conceptual trajectories of three grains, while panel (b) depicts the variance (8) is plotted for the parameters  $1/k_2 = 1.5$  with mean motion time 1.5 s,  $1/k_1 = 30.0$  resting time 30.0 s, and  $v = 0.1$  movement velocity 0.1 m/s. These values compare comparable to laboratory time-experiments transporting small ( $\sim 55$  mm) gravels (Lajeunesse et al., 2010; Martin et al., 2012). The timescale of burial timescale is set to  $1/\kappa = 7200.07200.0$  s (two hours), and the initial condition is grains start from rest ( $\theta_1 = 1$ ). The solid line is equation (8) while, and the points are numerically simulated. When  $k_2 \gg k_1 \gg \kappa$  as in this plot, there are Panel (b) demonstrates four distinct scaling ranges of  $\sigma_x^2$ : local, intermediate, global, and geomorphic. The first three are diffusive. Three crossover times  $\tau_L$ ,  $\tau_I$ , and  $\tau_G$  divide the ranges. Within each range, a slope key is added to demonstrate demonstrates the scaling  $\sigma_x^2 \propto t^\gamma$ . There are three crossovers between these ranges Panel (a) demonstrates that different mixtures of motion, denoted on rest, and burial states generate the figure by vertical lines ranges. At local timescales, grains usually either rest or move; at intermediate timescales, they transition between rest and labeled by motion; at global timescales  $\tau_L$ ,  $\tau_I$  they transition between rest, motion, and  $\tau_G$  burial; and at geomorphic timescales, all grains bury. These Additional slope keys in the local and global ranges of panel (b) illustrate the effect of initial conditions and rest/burial timescales depend on  $k_2$  the diffusion,  $k_1$  while the additional slope key within the geomorphic range demonstrates the expected scaling when burial is not permanent, and  $\kappa$  as we discuss in section 3.

241 ate a super-diffusive local range (S. Fathel et al., 2016; Martin et al., 2012; Witz,  
242 Cameron, & Nikora, 2019), a normal-diffusive intermediate range (Nakagawa & Tsu-



jimoto, 1976; Yano, 1969), and a super-diffusive global range (Bradley, 2017; Bradley, Tucker, & Benson, 2010), before the diffusion eventually terminates in a geomorphic range (Hassan & Bradley, 2017). Nikora et al. (2002) highlighted the need for such a physical description, although they suggested to use a two-state random walk between motion and rest states with heavy-tailed resting times, and they did not discuss sediment burial. ~~In the preliminary studies for this paper, we found~~ However, other works have demonstrated that a two-state walk with heavy-tailed rests provides two diffusion ranges – not three ~~– this conclusion is also suggested by and~~. ~~Although~~ (Fan et al., 2016; Weeks, Urbach, & Swinney, 1996), ~~and although~~ heavy-tailed ~~surface~~ resting times have been documented for surface particles (Fraccarollo & Hassan, 2019; Liu, Pelosi, & Guala, 2019), they are more often associated with ~~sediment burial, and surface resting times usually display light tails~~. These realizations and the need for a ~~physical model of three diffusion ranges led us to develop a three-state random walk for buried particles~~ (Martin et al., 2012, 2014; Olinde & Johnson, 2015; Pelosi, Schumer, Parker, & Ferguson, 2016; Pierce & Hassan, 2020; Voepel et al., 2013), while surface particles retain light-tailed resting times (Ancey et al., 2006; Einstein, 1937; Nakagawa & Tsujimoto, 1976; Yano, 1969). Accordingly, we developed a random walk model of bedload trajectories with light-tailed surface resting times ~~and that incorporates~~ sediment burial.

The local and intermediate range diffusion characteristics resulting from our model correspond closely to the original Nikora et al. concepts, while our global range has a different origin than Nikora et al. ~~described~~ envisioned. Nikora et al. (2001) explained that local diffusion results from the non-fractal (smooth) characteristics of bedload trajectories between subsequent interactions with the bed, while intermediate diffusion results from the fractal (rough) characteristics of bedload trajectories after many interactions with the bed. Our model represents these conclusions: non-fractal (and super-diffusive) bedload trajectories exist on timescales short enough that each grain is either resting or moving, while fractal (and normal-diffusive) bedload trajectories exist on timescales when grains are actively switching between motion and rest states. We conclude that local and intermediate ranges stem from the interplay between motion and rest timescales, as demonstrated by earlier two-state random walk models (Lajeunesse et al., 2018; Lisle et al., 1998) and by all Newtonian models that develop sequences of ~~rests and motions~~ motions and rests (Bialik et al., 2012; Nikora et al., 2001), even those including heavy-tailed rests (Fan et al., 2016).

### 3.2 Global and geomorphic ranges with next steps for research

Nikora et al. explained that divergent resting times generate a sub-diffusive global range. However, studies have demonstrated that ~~heavy-tailed~~ divergent resting times can generate super-diffusion in asymmetric random walks (Weeks & Swinney, 1998; Weeks et al., 1996), and both experiments (Bradley, 2017; Bradley et al., 2010) and models (Pelosi et al., 2016; Wu, Fofoula-Georgiou, et al., 2019; Wu, Singh, et al., 2019) of bedload tracers undergoing burial have demonstrated global range super-diffusion. While our results also show global range super-diffusion, they do not necessarily refute the Nikora et al. conclusion of sub-diffusion at large-long timescales. We assumed sediment burial was a permanent condition which developed ~~an extremely sub-diffusive geomorphic range~~  $(\gamma \rightarrow 0)$  a non-diffusive geomorphic range. In actuality, burial is a temporary condition ~~since~~, because bed scour can exhume buried sediment back into transport (Wu, Singh, et al., 2019), probably after heavy-tailed intervals (Martin et al., 2014; Pierce & Hassan, 2020; Voepel et al., 2013). We anticipate that a generalization of our model ~~including to include~~ heavy-tailed ~~intervals separating timescales between~~ burial and exhumation would develop four ranges of diffusion, ~~with where~~ the long-time decay of the exhumation time distribution would dictate the geomorphic range diffusion characteristics as depicted in figure 2. If cumulative exhumation times decay faster than  $T^{-1/2}$ , as suggested by equilibrium transport models (Martin et al.,

2014; Pierce & Hassan, 2020; Voepel et al., 2013) and laboratory experiments (Martin et al., 2012, 2014), we expect a super-diffusive geomorphic range (Weeks & Swinney, 1998). However, if they decay slower than  $T^{-1/2}$ , as implicitly suggested by the data of Olinde and Johnson (2015), we expect a genuinely sub-diffusive ~~sealing ( $0 < \gamma < 1$ )~~ in the geomorphic range (Weeks & Swinney, 1998), leaving Nikora et al. with the final word on long-time sub-diffusion.

The analytical solution of bedload diffusion in equation (8) reduces exactly to the analytical solutions of the Lisle et al. (1998) and Lajeunesse et al. (2018) models in the limit without burial ( $\kappa \rightarrow 0$ ), the Wu, Foufoula-Georgiou, et al. (2019) model in the limit of instantaneous steps ( $k_2 \rightarrow \infty$  and  $l = v/k_2$ ), and the original Einstein (1937) model in the limit of instantaneous steps without burial. These reductions demonstrate that the majority of recent bedload diffusion models, whether developed from Exner-type equations (Pelosi & Parker, 2014; Pelosi et al., 2016; Wu, Foufoula-Georgiou, et al., 2019) or advection-diffusion equations (Lajeunesse et al., 2018; Lisle et al., 1998), can be viewed equivalently as ~~continuous time~~ continuous-time random walks applied to individual bedload trajectories. Within random walk theory, sophisticated ~~mathematical~~ descriptions of transport with variable velocities (Masoliver & Weiss, 1994; Zaburdaev, Schmiedeberg, & Stark, 2008), correlated motions (Escaff, Toral, Van Den Broeck, & Lindenberg, 2018; Vicsek & Zafeiris, 2012), and anomalous diffusion (Fa, 2014; Masoliver, 2016; Metzler, Jeon, Cherstvy, & Barkai, 2014) have been developed. Meanwhile, in bedload transport research, variable velocities (Furbish et al., 2012; Heyman, Bohorquez, & Ancey, 2016; Lajeunesse et al., 2010), correlated motions (Heyman, Ma, Mettra, & Ancey, 2014; Lee & Jerolmack, 2018; Saletti & Hassan, 2020), and anomalous diffusion (Bradley, 2017; S. Fathel et al., 2016; Schumer et al., 2009) constitute open research issues. We believe further ~~exploiting~~ developing the linkage between existing bedload models and random walk concepts could rapidly progress our understanding ~~of these issues~~.

## 4 Conclusion

We developed a random walk model to describe sediment tracers transporting through a river channel as they gradually become buried, providing a physical description of the local, intermediate, and global diffusion ranges identified by Nikora et al. (2002). Pushing their ideas somewhat further, we proposed a geomorphic range to describe diffusion characteristics at timescales larger than the global range when burial and exhumation both moderate downstream transport. At base level, our model demonstrates that (1) durations of sediment motions, (2) durations of sediment rest, and (3) the sediment burial process are sufficient to develop three diffusion ranges that terminate when all tracers become buried. A next step is to incorporate exhumation to better understand the geomorphic range. Ultimately, we emphasize that the multi-state random walk formalism used in this paper implicitly underlies most existing bedload diffusion models and provides a ~~useful~~ powerful tool for researchers targeting landscape-scale understanding from statistical concepts of the underlying grain-scale dynamics.

## Acknowledgments

K. Pierce acknowledges thoughtful exchanges with Eduardo Daly and Eric Weeks during the early stages of this work. Both authors would like to thank Matteo Saletti, Conor McDowell, ~~Matteo Saletti~~ Shawn Chartrand, and Will Booker for helpful discussions. M. Hassan is supported by an NSERC Discovery grant. The Python simulation code is freely available at <https://zenodo.org/record/3659291#.Xj3p7XVKjIU>.

## References

- Ancey, C., Böhm, T., Jodeau, M., & Frey, P. (2006). Statistical description of sediment transport experiments. *Physical Review E - Statistical, Nonlinear, and Soft Matter Physics*, 74(1), 1–14. doi: 10.1103/PhysRevE.74.011302
- Arfken, G. (1985). *Mathematical methods for physicists*. Academic Press, Inc. doi: 10.1063/1.3062258
- Barik, D., Ghosh, P. K., & Ray, D. S. (2006). Langevin dynamics with dichotomous noise; Direct simulation and applications. *Journal of Statistical Mechanics: Theory and Experiment*(3). doi: 10.1088/1742-5468/2006/03/P03010
- Bialik, R. J., Nikora, V. I., Karpiński, M., & Rowiński, P. M. (2015). Diffusion of bedload particles in open-channel flows: distribution of travel times and second-order statistics of particle trajectories. *Environmental Fluid Mechanics*, 15(6), 1281–1292. doi: 10.1007/s10652-015-9420-5
- Bialik, R. J., Nikora, V. I., & Rowiński, P. M. (2012). 3D Lagrangian modelling of saltating particles diffusion in turbulent water flow. *Acta Geophysica*, 60(6), 1639–1660. doi: 10.2478/s11600-012-0003-2
- Bradley, D. N. (2017). Direct Observation of Heavy-Tailed Storage Times of Bed Load Tracer Particles Causing Anomalous Superdiffusion. *Geophysical Research Letters*, 44(24), 12,227–12,235. doi: 10.1002/2017GL075045
- Bradley, D. N., Tucker, G. E., & Benson, D. A. (2010). Fractional dispersion in a sand bed river. *Journal of Geophysical Research*, 115, F00A09. Retrieved from <http://doi.wiley.com/10.1029/2009JF001268> doi: 10.1029/2009jf001268
- Cundall, P. A., & Strack, O. D. (1979). A discrete numerical model for granular assemblies. *Geotechnique*, 29(1), 47–65. Retrieved from <http://www.icervirtuallibrary.com/doi/10.1680/geot.1979.29.1.47> doi: 10.1680/geot.1979.29.1.47
- Einstein, H. A. (1937). *Bed load transport as a probability problem*. (English translation by W. W. Sayre, in Sedimentation, edited by H. W. Shen, Appendix C, Fort Collins, Colo., 1972.).
- Escaff, D., Toral, R., Van Den Broeck, C., & Lindenberg, K. (2018). A continuous-time persistent random walk model for flocking. *Chaos*, 28(7), 1–11. doi: 10.1063/1.5027734
- Ettema, R., & Mutel, C. F. (2014). *Hans Albert Einstein: his life as a pioneering engineer* (Vol. 54) (No. 3). ASCE Press. doi: 10.1080/00221686.2016.1165295
- Fa, K. S. (2014). Uncoupled continuous-time random walk model: Analytical and numerical solutions. *Physical Review E - Statistical, Nonlinear, and Soft Matter Physics*, 89(5), 1–9. doi: 10.1103/PhysRevE.89.052141
- Fan, N., Singh, A., Guala, M., Foufoula-Georgiou, E., & Wu, B. (2016). Exploring a semimechanistic episodic Langevin model for bed load transport: Emergence of normal and anomalous advection and diffusion regimes. *Water Resources Research*, 52(4), 2789–2801. doi: 10.1002/2016WR018704. Received
- Fathel, S., Furbish, D., & Schmeeckle, M. (2016). Parsing anomalous versus normal diffusive behavior of bedload sediment particles. *Earth Surface Processes and Landforms*, 41(12), 1797–1803. doi: 10.1002/esp.3994
- Fathel, S. L., Furbish, D. J., & Schmeeckle, M. W. (2015). Experimental evidence of statistical ensemble behavior in bed load sediment transport. *Journal of Geophysical Research F: Earth Surface*, 120(11), 2298–2317. doi: 10.1002/2015JF003552
- Ferguson, R. I., Bloomer, D. J., Hoey, T. B., & Werritty, A. (2002). Mobility of river tracer pebbles over different timescales. *Water Resources Research*, 38(5), 3–1–3–8. doi: 10.1029/2001wr000254
- Ferguson, R. I., & Hoey, T. B. (2002). Long-term slowdown of river tracer pebbles: Generic models and implications for interpreting short-term tracer studies. *Water Resources Research*, 38(8), 17–1–17–11. doi: 10.1029/2001wr000637
- Fraccarollo, L., & Hassan, M. A. (2019). Einstein conjecture and resting-Time statis-

- tics in the bed-load transport of monodispersed particles. *Journal of Fluid Mechanics*, 876, 1077–1089. doi: 10.1017/jfm.2019.563
- Furbish, D. J., Ball, A. E., & Schmeeckle, M. W. (2012). A probabilistic description of the bed load sediment flux: 4. Fickian diffusion at low transport rates. *Journal of Geophysical Research: Earth Surface*, 117(3), 1–13. doi: 10.1029/2012JF002356
- Furbish, D. J., Fathel, S. L., Schmeeckle, M. W., Jerolmack, D. J., & Schumer, R. (2017). The elements and richness of particle diffusion during sediment transport at small timescales. *Earth Surface Processes and Landforms*, 42(1), 214–237. doi: 10.1002/esp.4084
- Gaeuman, D., Stewart, R., Schmandt, B., & Pryor, C. (2017). Geomorphic response to gravel augmentation and high-flow dam release in the Trinity River, California. *Earth Surface Processes and Landforms*, 42(15), 2523–2540. doi: 10.1002/esp.4191
- Gordon, R., Carmichael, J. B., & Isackson, F. J. (1972). Saltation of plastic balls in a onedimensional flume. *Water Resources Research*, 8(2), 444–459. doi: 10.1029/WR008i002p00444
- Haschenburger, J. K. (2013). Tracing river gravels: Insights into dispersion from a long-term field experiment. *Geomorphology*, 200, 121–131. Retrieved from <http://dx.doi.org/10.1016/j.geomorph.2013.03.033> doi: 10.1016/j.geomorph.2013.03.033
- Hassan, M. A., & Bradley, D. N. (2017). Geomorphic controls on tracer particle dispersion in gravel-bed rivers. In D. Tsutsumi & J. B. Laronne (Eds.), *Gravel-bed rivers 8: Processes and disasters* (1st ed.). John Wiley & Sons Ltd. doi: 10.1002/9781118971437.ch6
- Hassan, M. A., & Church, M. (1994). Vertical mixing of coarse particles in gravel bed rivers: A kinematic model. *Water Resources Research*, 30(4), 1173–1185. doi: 10.1029/93WR03351
- Hassan, M. A., Church, M., & Schick, A. P. (1991). Distance of movement of coarse particles in gravel bed streams. *Water Resources Research*, 27(4), 503–511. doi: 10.1029/90WR02762
- Hassan, M. A., Voepel, H., Schumer, R., Parker, G., & Fraccarollo, L. (2013). Displacement characteristics of coarse fluvial bed sediment. *Journal of Geophysical Research: Earth Surface*, 118(1), 155–165. doi: 10.1029/2012JF002374
- Heyman, J., Bohorquez, P., & Ancey, C. (2016). Entrainment, motion, and deposition of coarse particles transported by water over a sloping mobile bed. *Journal of Geophysical Research: Earth Surface*, 121(10), 1931–1952. doi: 10.1002/2015JF003672
- Heyman, J., Ma, H. B., Mettra, F., & Ancey, C. (2014). Spatial correlations in bed load transport: Evidence, importance, and modeling. *Journal of Geophysical Research: Earth Surface*, 119, 1751–1767. doi: 10.1002/2013JF003003. Received
- Hubbell, D., & Sayre, W. (1964). Sand Transport Studies with Radioactive Tracers. *Journal of the Hydraulics Division*, 90(3), 39–68.
- Kraichnan, R. H. (1970). Diffusion by a Random Velocity Field. *Physics of Fluids*, 13(1), 22. Retrieved from <http://scitation.aip.org/content/aip/journal/pof1/13/1/10.1063/1.1692799> doi: 10.1063/1.1692799
- Lajeunesse, E., Devauchelle, O., & James, F. (2018). Advection and dispersion of bed load tracers. *Earth Surface Dynamics*, 6(November), 389–399. doi: 10.5194/esurf-6-389-2018
- Lajeunesse, E., Malverti, L., & Charru, F. (2010). Bed load transport in turbulent flow at the grain scale: Experiments and modeling. *Journal of Geophysical Research: Earth Surface*, 115(4). doi: 10.1029/2009JF001628
- Lee, D. B., & Jerolmack, D. (2018). Determining the scales of collective entrainment in collision-driven bed load. *Earth Surface Dynamics*, 6(4), 1089–1099. doi: 10

- .5194/esurf-6-1089-2018
- Lisle, I. G., Rose, C. W., Hogarth, W. L., Hairsine, P. B., Sander, G. C., & Parlange, J.-Y. (1998). Stochastic sediment transport in soil erosion. *Journal of Hydrology*, 204, 217–230.
- Liu, M. X., Pelosi, A., & Guala, M. (2019). A Statistical Description of Particle Motion and Rest Regimes in Open-Channel Flows Under Low Bedload Transport. *Journal of Geophysical Research: Earth Surface*, 2666–2688. doi: 10.1029/2019JF005140
- Macklin, M. G., Brewer, P. A., Hudson-Edwards, K. A., Bird, G., Coulthard, T. J., Dennis, I. A., . . . Turner, J. N. (2006). A geomorphological approach to the management of rivers contaminated by metal mining. *Geomorphology*, 79(3-4), 423–447. doi: 10.1016/j.geomorph.2006.06.024
- Marcum, J. I. (1960). A Statistical Theory of Target Detection By Pulsed Radar. *IRE Transactions on Information Theory*, 6(2), 59–267. doi: 10.1109/TIT.1960.1057560
- Martin, R. L., Jerolmack, D. J., & Schumer, R. (2012). The physical basis for anomalous diffusion in bed load transport. *Journal of Geophysical Research: Earth Surface*, 117(1), 1–18. doi: 10.1029/2011JF002075
- Martin, R. L., Purohit, P. K., & Jerolmack, D. J. (2014). Sedimentary bed evolution as a mean-reverting random walk: Implications for tracer statistics. *Geophysical Research Letters*, 41(17), 6152–6159. doi: 10.1002/2014GL060525
- Masoliver, J. (2016). Fractional telegrapher’s equation from fractional persistent random walks. *Physical Review E*, 93(5), 1–10. doi: 10.1103/PhysRevE.93.052107
- Masoliver, J., & Weiss, G. H. (1994). Telegrapher’s equations with variable propagation speeds. *Physical Review E*, 49(5), 3852–3854. doi: 10.1103/PhysRevE.49.3852
- Metzler, R., Jeon, J. H., Cherstvy, A. G., & Barkai, E. (2014). Anomalous diffusion models and their properties: Non-stationarity, non-ergodicity, and ageing at the centenary of single particle tracking. *Physical Chemistry Chemical Physics*, 16(44), 24128–24164. doi: 10.1039/c4cp03465a
- Metzler, R., & Klafter, J. (2000). The random walk’s guide to anomalous diffusion: A fractional dynamics approach. *Physics Report*, 339(1), 1–77. doi: 10.1016/S0370-1573(00)00070-3
- Montroll, E. W., & Weiss, G. H. (1965). Random walks on lattices. *Journal of Mathematical Physics*, 6(167), 193–220. doi: 10.1090/psapm/016/0161378
- Nakagawa, H., & Tsujimoto, T. (1976). On probabilistic characteristics of motion of individual sediment particles on stream beds. In *Hydraulic problems solved by stochastic methods: Second international iahr symposium on stochastic hydraulics* (pp. 293–320). Lund, Sweden.
- Nakagawa, H., & Tsujimoto, T. (1980). Sand bed instability due to bed load motion. *Journal of Hydraulic Engineering*, 106(12), 2023–2051.
- Nikora, V., Habersack, H., Huber, T., & McEwan, I. (2002). On bed particle diffusion in gravel bed flows under weak bed load transport. *Water Resources Research*, 38(6), 17–1–17–9. Retrieved from <http://doi.wiley.com/10.1029/2001WR000513> doi: 10.1029/2001wr000513
- Nikora, V., Heald, J., Goring, D., & McEwan, I. (2001). Diffusion of saltating particles in unidirectional water flow over a rough granular bed. *Journal of Physics A: Mathematical and General*, 34(50). doi: 10.1088/0305-4470/34/50/103
- Olinde, L., & Johnson, J. P. L. (2015). Using RFID and accelerometer-embedded tracers to measure probabilities of bed load transport, step lengths, and rest times in a mountain stream. *Water Resources Research*, 51, 7572–7589. doi: 10.1002/2014WR016259
- Paintal, A. S. (1971). A stochastic model of bed load transport. *Journal of Hydraulic Research*, 9(4), 527–554. doi: 10.1080/00221687109500371



- Papangelakis, E., & Hassan, M. A. (2016). The role of channel morphology on the mobility and dispersion of bed sediment in a small gravel-bed stream. *Earth Surface Processes and Landforms*, 41(15), 2191–2206. doi: 10.1002/esp.3980
- Pelosi, A., & Parker, G. (2014). Morphodynamics of river bed variation with variable bedload step length. *Earth Surface Dynamics*, 2(1), 243–253. doi: 10.5194/esurf-2-243-2014
- Pelosi, A., Schumer, R., Parker, G., & Ferguson, R. I. (2016). The cause of advective slowdown of tracer pebbles in rivers: Implementation of Exner-Based Master Equation for coevolving streamwise and vertical dispersion. *Journal of Geophysical Research: Earth Surface*, 121, 623–637. doi: 10.1002/2014JF003184
- Phillips, C. B., Martin, R. L., & Jerolmack, D. J. (2013). Impulse framework for unsteady flows reveals superdiffusive bed load transport. *Geophysical Research Letters*, 40(7), 1328–1333. doi: 10.1002/grl.50323
- Pierce, J. K., & Hassan, M. A. (2020). Joint stochastic bedload transport and bed elevation model: variance regulation and power law rests. *Journal of Geophysical Research: Earth Surface*, 125(4), 1–15. doi: 10.1029/2019jf005259
- Prudnikov, A. P., Brychov, Y. A., Marichev, O. I., Brychkov, Y. A., Marichev, O. I., & Romer, R. H. (1986). *Integrals and Series* (Vol. 5) (No. 10). New York: Gordon and Breach. doi: 10.1119/1.15375
- Roseberry, J. C., Schmeeckle, M. W., & Furbish, D. J. (2012). A probabilistic description of the bed load sediment flux: 2. Particle activity and motions. *Journal of Geophysical Research: Earth Surface*, 117(3). doi: 10.1029/2012JF002353
- Saletti, M., & Hassan, M. A. (2020). Width variations control the development of grain structuring in steep step-pool dominated streams : insight from flume experiments. *Earth Surface Processes and Landforms*, 4815. doi: 10.1002/esp.4815
- Schmidt, M. G., Sagués, F., & Sokolov, I. M. (2007). Mesoscopic description of reactions for anomalous diffusion: A case study. *Journal of Physics Condensed Matter*, 19(6). doi: 10.1088/0953-8984/19/6/065118
- Schumer, R., Meerschaert, M. M., & Baeumer, B. (2009). Fractional advection-dispersion equations for modeling transport at the Earth surface. *Journal of Geophysical Research: Earth Surface*, 114(4), 1–15. doi: 10.1029/2008JF001246
- Sekine, M., & Kikkawa, H. (1992). Mechanics of saltating grains. II. *Journal of Hydraulic Engineering*, 118(4), 536–558. doi: 10.1061/(ASCE)0733-9429(1992)118:4(536)
- Shlesinger, M. F. (1974). Asymptotic solutions of continuous-time random walks. *Journal of Statistical Physics*, 10(5), 421–434. doi: 10.1007/BF01008803
- Sokolov, I. M. (2012). Models of anomalous diffusion in crowded environments. *Soft Matter*, 8(35), 9043–9052. doi: 10.1039/c2sm25701g
- Taylor, G. I. (1920). Diffusion by continuous movements. *Proceedings of the London Mathematical Society*, s2-20(1), 196–212. doi: 10.1063/1.1691776
- Temme, N. M. (1996). *Special Functions: An Introduction to the Classical Functions of Mathematical Physics*. John Wiley & Sons Ltd. doi: 10.1119/1.18604
- Vicsek, T., & Zafeiris, A. (2012, aug). Collective motion. *Physics Reports*, 517(3-4), 71–140. Retrieved from [www.elsevier.com/locate/physrep](http://www.elsevier.com/locate/physrep) doi: 10.1016/j.physrep.2012.03.004
- Voepel, H., Schumer, R., & Hassan, M. A. (2013). Sediment residence time distributions: Theory and application from bed elevation measurements. *Journal of Geophysical Research: Earth Surface*, 118(4), 2557–2567. doi: 10.1002/jgrf.20151
- Weeks, E. R., & Swinney, H. L. (1998). Anomalous diffusion resulting from strongly asymmetric random walks. *Physical Review E - Statistical Physics, Plasmas, Fluids, and Related Interdisciplinary Topics*, 57(5), 4915–4920. doi: 10.1103/

PhysRevE.57.4915

- Weeks, E. R., Urbach, J., & Swinney, H. L. (1996). Anomalous diffusion in asymmetric random walks with a quasi-geostrophic flow example. *Physica D: Nonlinear Phenomena*, 97, 291–310.
- Weiss, G. H. (1976). The two-state random walk. *Journal of Statistical Physics*, 15(2), 157–165. doi: 10.1007/BF01012035
- Weiss, G. H. (1994). *Aspects and Applications of the Random Walk*. Amsterdam: North Holland.
- Witz, M. J., Cameron, S., & Nikora, V. (2019). Bed particle dynamics at entrainment. *Journal of Hydraulic Research*, 57(4), 464–474. Retrieved from <https://doi.org/10.1080/00221686.2018.1489898> doi: 10.1080/00221686.2018.1489898
- Wu, Z., Foufoula-Georgiou, E., Parker, G., Singh, A., Fu, X., & Wang, G. (2019). Analytical Solution for Anomalous Diffusion of Bedload Tracers Gradually Undergoing Burial. *Journal of Geophysical Research: Earth Surface*, 124(1), 21–37. doi: 10.1029/2018JF004654
- Wu, Z., Singh, A., Fu, X., & Wang, G. (2019). Transient Anomalous Diffusion and Advective Slowdown of Bedload Tracers by Particle Burial and Exhumation. *Water Resources Research*, 7964–7982. doi: 10.1029/2019WR025527
- Yang, C. T., & Sayre, W. (1971). Stochastic Model for Sand Dispersion. *Journal of the Hydraulics Division*, 97(2), 265–288.
- Yano, K. (1969). Tracer Studies on the Movement of Sand and Gravel. In *Proceedings of the 12th congress iahr, vol 2*. (pp. 121–129). Kyoto, Japan.
- Zaburdaev, V., Schmiedeberg, M., & Stark, H. (2008). Random walks with random velocities. *Physical Review E - Statistical, Nonlinear, and Soft Matter Physics*, 78(1), 1–5. doi: 10.1103/PhysRevE.78.011119
- Zhang, Y., Meerschaert, M. M., & Packman, A. I. (2012). Linking fluvial bed sediment transport across scales. *Geophysical Research Letters*, 39(20), 1–6. doi: 10.1029/2012GL053476